Mitzscherling, J., Winkel, M., Winterfeld, M., Horn, F., Yang, S., Grigoriev, M. N., Wagner, D., Overduin, P. P., Liebner, S. (2017): The development of permafrost bacterial communities under submarine conditions. - *Journal of Geophysical Research*, *122*, 7, pp. 1689—1704.

DOI: http://doi.org/10.1002/2017JG003859

AGU PUBLICATIONS

JGR

Journal of Geophysical Research: Biogeosciences

RESEARCH ARTICLE
10.1002/2017JG003859

Special Section:
The Arctic: An AGU Joint Special Collection

The development of permafrost bacterial communities under submarine conditions

Julia Mitzscherling[1], Matthias Winkel[1], Maria Winterfeld[2,3], Fabian Horn[1], Sizhong Yang[1], Mikhail N. Grigoriev[4], Dirk Wagner[1], Pier P. Overduin[2], and Susanne Liebner[1]

[1]GFZ German Research Centre for Geosciences, Section 5.3 Geomicrobiology, Potsdam, Germany, [2]Helmholtz Centre for Polar and Marine Research, Research Department Potsdam, Alfred Wegener Institute, Potsdam, Brandenburg, Germany, [3]Now at Helmholtz Centre for Polar and Marine Research, Research Department Bremerhaven, Alfred Wegener Institute, Bremerhaven, Bremen, Germany, [4]Melnikov Permafrost Institute, Siberian Branch, Russian Academy of Sciences, Yakutsk, Russia

Key Points:
- Submarine permafrost is an extreme habitat for microbial life deep below the seafloor with changing thermal and chemical conditions
- Millennia after inundation by seawater, bacteria stratify into communities in permafrost, marine-affected permafrost, and seabed sediments
- Permafrost pore water chemistry changes in response to inundation before permafrost thaws; it can be used to detect the marine influence

Supporting Information:
- Supporting Information S1
- Table S1

Correspondence to:
J. Mitzscherling,
jmagritz@gfz-potsdam.de

Citation:
Mitzscherling, J., M. Winkel, M. Winterfeld, F. Horn, S. Yang, M. N. Grigoriev, D. Wagner, P. P. Overduin, and S. Liebner (2017), The development of permafrost bacterial communities under submarine conditions, *J. Geophys. Res. Biogeosci.*, *122*, 1689–1704, doi:10.1002/2017JG003859.

Received 23 MAR 2017
Accepted 16 JUN 2017
Accepted article online 21 JUN 2017
Published online 17 JUL 2017

Abstract Submarine permafrost is more vulnerable to thawing than permafrost on land. Besides increased heat transfer from the ocean water, the penetration of salt lowers the freezing temperature and accelerates permafrost degradation. Microbial communities in thawing permafrost are expected to be stimulated by warming, but how they develop under submarine conditions is completely unknown. We used the unique records of two submarine permafrost cores from the Laptev Sea on the East Siberian Arctic Shelf, inundated about 540 and 2500 years ago, to trace how bacterial communities develop depending on duration of the marine influence and pore water chemistry. Combined with geochemical analysis, we quantified total cell numbers and bacterial gene copies and determined the community structure of bacteria using deep sequencing of the bacterial 16S rRNA gene. We show that submarine permafrost is an extreme habitat for microbial life deep below the seafloor with changing thermal and chemical conditions. Pore water chemistry revealed different pore water units reflecting the degree of marine influence and stages of permafrost thaw. Millennia after inundation by seawater, bacteria stratify into communities in permafrost, marine-affected permafrost, and seabed sediments. In contrast to pore water chemistry, the development of bacterial community structure, diversity, and abundance in submarine permafrost appears site specific, showing that both sedimentation and permafrost thaw histories strongly affect bacteria. Finally, highest microbial abundance was observed in the ice-bonded seawater unaffected but warmed permafrost of the longer inundated core, suggesting that permafrost bacterial communities exposed to submarine conditions start to proliferate millennia after warming.

1. Introduction

Extensive shallow water areas of the Arctic continental shelf are underlain by submarine permafrost [*Zhang et al.,* 1999; *Rachold et al.,* 2007]. The shallowest and most spacious shelf of the World Ocean is the East Siberian Arctic Shelf encompassed by the Laptev, East Siberian, and the Russian part of the Chukchi Seas. It comprises more than 80% of the potential submarine permafrost in the Arctic [*Overduin et al.,* 2015].

Submarine permafrost is relict terrestrial permafrost that developed on land and was subsequently inundated by postglacial sea level rise during the Holocene, 7 to 15 ka ago [*Romanovskii and Hubberten,* 2001]. Even today, especially Arctic permafrost coasts, which account for 34% of the coasts worldwide [*Lantuit et al.,* 2012], are vulnerable to sea level rise, declining sea ice cover, and longer and warmer thawing seasons [*Fritz et al.,* 2017]. Resulting coastline collapses, with mean modern erosion rates of 1 to 2 m yr^{-1} [*Lantuit et al.,* 2012] and local erosion rates of up to 25 m y^{-1} [*Jones et al.,* 2009], lead to an annual formation of about 10 km^2 of submarine permafrost on the East Siberian Arctic Shelf alone [*Grigoriev*, 2008]. This erosion of permafrost coasts is an abrupt form of permafrost degradation and results in yet unquantified fluxes of carbon and nutrients from thawing permafrost with presumably large consequences for the biogeochemical cycling of the shelf area [*Fritz et al.,* 2017].

The seawater inundation and infiltration cause drastic changes in the thermal regime and geochemical composition of submarine permafrost [*Ulyantsev et al.,* 2016]. With annual average bottom water temperatures of −1.8°C to −1°C [*Wegner et al.,* 2005], it is 12 to 17°C warmer than the annual average surface temperature over on-land permafrost [*Romanovskii et al.,* 2005]. As temperatures in high latitudes have been rising faster than the global average over the past decades [*IPCC,* 2013], bottom water warming further increases

the degradation rates of submarine permafrost in the Laptev and East Siberian Seas. Besides top-down seawater heat and salt fluxes, bottom-up geothermal heat fluxes are responsible for the degradation of submarine permafrost [*Osterkamp*, 2001; *Shakhova et al.,* 2010]. The seabed temperature of much of the Arctic shelf seas is cryotic (<0°C). In coastal waters, submarine permafrost temperature is around −1°C [*Overduin et al.,* 2015], the limit to maintain ice-bonded permafrost under submarine conditions [*Grigoriev*, 2008]. Warming and destabilization of submarine permafrost increase sediment permeability. On the one hand, this can result in the release of long preserved methane (CH_4) into the water column and atmosphere [*Shakhova et al.,* 2010; *Portnov et al.,* 2013; *Shakhova et al.,* 2014, *Thornton et al.,* 2016]. On the other hand, trapped organic material becomes more accessible to microorganisms after thawing, potentially inducing the decomposition of soil organic matter and transforming complex organic compounds to soluble metabolites and gases, such as CH_4, CO_2, and N_2O [*Graham et al.,* 2012; *Mackelprang et al.,* 2011]. Its release is potentially relevant to global climate, since terrestrial and submarine permafrost store twice as much carbon as is currently in the atmosphere [*Schuur et al.,* 2009].

Microbial life in thawing permafrost is expected to be stimulated before permafrost thaws completely [*Schuur et al.,* 2015]; i.e., activity and abundance should increase [*Waldrop et al.,* 2010; *Graham et al.,* 2012; *Mackelprang et al.,* 2011]. Submarine permafrost is thereby affected not only by rising temperatures but also by elevated salt concentrations [*Harrison and Osterkamp*, 1982]. In particular, during the first decades of inundation, there may be an active layer at the seabed that thaws and freezes seasonally [*Osterkamp*, 2001]. Brine drainage from the growing sea ice increases water salinity and decreases temperatures of the bottom-water in fall and winter. Brines can infiltrate the seabed, even when it is frozen. They are responsible for thawing the underlying submarine permafrost at negative sediment temperatures. In contrast to rising temperatures and the release of substrate, the evolution of submarine permafrost with salt infiltration as the main process has been disregarded in assumptions how microbial life responds to submarine permafrost thaw. Osmotic stress is known to limit microbial growth and activity [*Galinski,* 1995]. Although microbes have a number of features (fast growth rates, physiological flexibility, and a rapid evolution, i.e., mutation or horizontal gene transfer) to acclimate, adapt, and recover, several studies showed that microbial community composition is sensitive to disturbances [reviewed by *Allison and Martiny,* 2008]. These studies observed shifts and no resilience in the microbial community composition within a few years. Therefore, we hypothesize that increasing salinity in terrestrial permafrost deposits might impair the indigenous microbial community before it is stimulated through rising temperatures. We expect the terrestrial community to change its composition in response to seawater infiltration. Assuming limited microbial growth and activity due to osmotic stress, as mentioned above, the community is initially expected to decrease in population size. To test this, we studied the pore water chemistry and bacterial community composition, diversity, and abundance by means of the bacterial 16S rRNA gene copy numbers, total cell counts, and deep sequencing of the bacterial 16S rRNA gene of two submarine permafrost cores from the Western and Central Laptev Sea Shelf inundated for different time periods.

2. Materials and Methods

2.1. Regional Setting and Study Areas

The Laptev Sea, bordered by the Taymyr Peninsula to the west and the New Siberian Island to the east, has an average water depth of less than 60 m. During the Weichselian glaciation (Late Pleistocene), large areas of the nonglaciated arctic continental shelf were exposed to climatic conditions which led to the formation of cold, thick, and continuous permafrost [*Svendsen et al.,* 2004]. Subsequently, a large portion of the ice-rich terrestrial permafrost that developed was inundated by a combination of the Holocene marine transgression and coastal thermoerosion [*Winterfeld et al.,* 2011].

The first study area at Cape Mamontov Klyk (supporting information Figure S1) was described by *Winterfeld et al.* [2011]. Cape Mamontov Klyk (~73°60′N, 117°18′E) is situated in the Western Laptev Sea. During a campaign in 2005 [*Rachold et al.,* 2007; *Schirrmeister*, 2007], a submarine core (C2) was drilled about 11.5 km offshore. Assuming a mean annual coastal erosion rate of 4.5 m yr^{-1} [*Grigoriev*, 2008], the drill site was inundated 2500 years ago [*Rachold et al.,* 2007]. The core was retrieved in approximately 6 m water depth with a sea ice thickness of 1.35 m and bottom-water salinity of 29.2 practical salinity unit (psu). Core material was retrieved between 6 and 77 m bsl (meters below sea level). Temperature measurements at the site of C2

were performed 1 to 11 days after drilling and are described and published elsewhere [*Junker et al.,* 2008; *Overduin et al.,* 2008]. Temperatures of the C2 borehole ranged between −1.5 and −0.8°C.

The second study area is located in the Buor Khaya Bay (supporting information Figure S1). Within the framework of the Drilling Expedition Buor Khaya in 2012 [*Günther et al.,* 2013], the submarine sediment core BK2 was retrieved about 750 m off the coast west of the Buor Khaya Peninsula, in the Central Laptev Sea. Drilling was performed in 4.3 m deep water with a sea ice cover of 2.09 m and a bottom-water salinity of 5.9 psu [*Günther et al.,* 2013]. Core material was retrieved between 6 and 51 m bsl. Borehole temperature of BK2 was recorded for 4 days after drilling. Measurement and temperature data of BK2 were published by *Overduin et al.* [2015]. Borehole temperatures ranged between 0.4 and −0.9°C. Based on the distance of the borehole from the modern coastline and on the mean annual erosion rate of 1.4 ± 0.8 m yr^{-1} [*Günther et al.,* 2012], the location of BK2 was flooded around 540 years ago [*Overduin et al.,* 2015]. Since the Buor Khaya Peninsula is covered by thermokarst depressions and characterized by an eroding Ice Complex coastal bluff, it is likely that the drill site was affected by Holocene thermokarst or thermokarst lake development prior to erosion and that it was frozen at the time of inundation.

2.2. Geochemical Analyses

Pore water was extracted from thawed subsamples of the sediment cores using Rhizons™ (0.2 μm pore diameter). Electrical conductivity, salinity, cation (Ba^{2+}, Ca^{2+}, K^+, Mg^{2+}, Na^+, and Si_{aq}) and anion (Cl^-, SO_4^{2-}, Br^-, NO_3^-) concentrations, stable isotope concentrations ($\delta^{18}O$ and δD), and pH were measured for 94 samples of C2 (Cape Mamontov Klyk) and for 80 samples of BK2 (Buor Khaya Bay; supporting information Tables S1 and S2). Electrical conductivity and salinity were measured with a WTW MultiLab 540 by using a standard conductivity cell (TetraConR 325) with four graphite electrodes. Total dissolved element concentration was determined via the analytical technique of inductively coupled plasma optical emission spectrometry using a Perkin-Elmer ICP-OES Optima 3000XL. In order to measure the concentration (mg/L) of dissolved anions, an ion chromatograph (Dionex DX-320), a latex-particle separation column, and KOH as eluent were used. Values below detection limit were assigned values of half the detection limit for inclusion in principal component analyses (PCAs). The determination of deuterium (δD) and oxygen isotope ($\delta^{18}O$) ratios was performed using a Finnigan MAT Delta-S mass spectrometer in combination with two equilibration units (MS Analysetechnik, Berlin).

2.3. Extraction of Nucleic Acids

Total nucleic acids were extracted as described by *Zhou et al.* [1996] in a slightly modified way. Sediment samples from 5 to 10 g were homogenized in liquid nitrogen and mixed with 13.5 mL of DNA extraction buffer (100 m*M* Tris-HCl [pH 8.0], 100 m*M* sodium EDTA [pH 8.0], 100 m*M* sodium phosphate [pH 8.0], and 1.5 *M* NaCl, 1% CTAB) and 100 μL of proteinase K (10 mg/mL) in 50 mL centrifuge tubes. They were incubated with horizontal shaking for 1 h at 37°C and 225 rpm. After the addition of 1.5 mL of 20% sodium dodecyl sulfate, the samples were incubated in a water bath at 65°C for 2 h with gentle inversions every 20 min. Supernatants were recovered by centrifugation at 6000 *g* for 10 min at room temperature and collected in fresh 50 mL centrifuge tubes. The sediment pellets were extracted two more times as follows: addition of 4.5 mL of extraction buffer and 0.5 mL of 20% sodium dodecyl sulfate, vortexing the tubes for 10 s, incubation at 65°C for 10 min, and centrifugation as described before. Supernatants of the three extraction cycles were combined and mixed with an equal volume of chloroform-isoamyl alcohol (24:1 vol/vol) and the coprecipitant GlycoBlue™ (1:300). After recovery of the aqueous phase by centrifugation, the DNA was precipitated with 0.6 volumes of isopropanol at room temperature for 1 h and pelleted by centrifugation at 16,000 *g* for 20 min. Finally, the DNA pellet was washed three times with 1 mL of ice-cold 70% ethanol and resuspended in a final volume of 500 μL of sterile deionized water.

Genomic DNA was quantified with the QBIT2 system (Invitrogen, HS-quant DNA) and calculated per gram sediment wet weight. The crude DNA was purified using the HiYield PCR Clean-Up and Gel-Extraction Kit (Südlabor, Gauting, Germany) to reduce polymerase chain reaction (PCR) inhibitors and the necessity to dilute the DNA extracts prior to PCR applications.

2.4. Quantification of the Bacterial 16S rRNA Genes

Quantitative PCR was performed using the CFX Connect™ Real-Time PCR Detection System (Bio-Rad Laboratories, Inc., Hercules, USA) and the following primer set: Eub341F and Eub534R [*Muyzer et al.,* 1993].

Each reaction (25 μL) contained 2× concentrate of iTaq™ Universal SYBR® Green Supermix (Bio-Rad Laboratories, Inc., Hercules, USA), 0.4 μ*M* of the forward and reverse primer, sterile water, and 5 μL of DNA template. The environmental DNA samples were diluted 5- to 100-fold and run in three technical replicates. The PCR reactions comprised an initial denaturation (5 min at 95°C), followed by 40 cycles of 0.5 s at 95°C, 30 s at an annealing temperature of 55.7°C, 10 s at 72°C, and a plate read step at 80°C for 0.3 s. Melt curve analysis from 65 to 95°C with 0.5°C temperature increment per 0.5 s cycle and gel electrophoresis on the PCR products were conducted at the end of each run to identify nonspecific amplification of DNA. The qPCR assay was calibrated using known amounts of PCR amplified and cloned gene fragments from a pure *Escherichia coli* culture. Genomic standards were included in each qPCR run to ensure linearity and expected slope values of the Ct/log curves. PCR efficiency**,** based on the standard curve, was calculated using the BioRad CFX Manager software and varied between 95 and 100%. All cycle data were collected using the single threshold Cq determination mode. Abundances of the bacterial 16S rRNA gene and of cells were calculated per gram sediment wet weight.

2.5. Amplification and Illumina MiSeq Sequencing of the Bacterial 16S rRNA Gene

We sequenced 19 samples from the core C2 and 10 samples from BK2. From BK2, two samples right above and below the ice-bonded permafrost table were pooled. The sampling depths are illustrated in Figure 2. PCR and sequencing were performed in two technical replicates for each sample. Bacterial 16S rRNA genes were amplified using the sequencing primers S-D-Bact-0341-b-S-17 and S-D-Bact-0785-a-A-21 (supporting information Table S3) comprising different combinations of barcodes (supporting information Table S4). Preparation and sequencing was performed in two technical replicates.

The PCR amplification was carried out with a T100™ Thermal Cycler (Bio-Rad Laboratories, CA, USA), and the PCR mixture of 25 μL contained 0.025 U μL^{-1} of HotStarTaq DNA Polymerase (Qiagen), 1× PCR buffer (Tris-Cl, KCl, $(NH_4)_2SO_4$, 15 m*M* $MgCl_2$; pH 8.7, Qiagen), 0.4 μ*M* of forward and reverse primer (supporting information Table S3), dNTP mix (0.2 m*M* each; Thermo Fisher Scientific, Darmstadt, Germany), 2 μ*M* of $MgCl_2$ (Qiagen), RNase-free water (EURx), and 2.5 μL of DNA extract. PCR conditions were as follows: initial denaturation at 95°C for 5 min, followed by 30 cycles of denaturation (95°C for 30 s), annealing (55°C for 30 s) and elongation (72°C for 1 min), and a final extension step of 72°C for 10 min.

The PCR products were purified from agarose gel with the HiYieldPCR Clean-Up and Gel-Extraction Kit (Südlabor, Gauting, Germany). Amplicons were quantified with the QBIT2 system (Invitrogen, HS-Quant DNA), mixed in equimolar amounts and sequenced from both directions (GATC Biotech, Konstanz) based on the Illumina MiSeq technology. The library was prepared with the MiSeq Reagent Kit V3 for 2× 300 bp paired-end reads according to the manufacturer's protocols. For better performance due to different sequencing length, 15% PhiX control v3 library was used.

2.6. Sequence Analyses and Bioinformatics

The acquired raw data of bacterial sequences were analyzed starting with the quality control of the sequencing library by the tool FastQC (Quality Control tool for High Throughput Sequence Data http://www.bioinformatics.babraham.ac.uk/projects/fastqc/ by S. Andrews). Demultiplexing of the sequence reads according to their barcodes and subsequent removal of the barcodes were performed with the CutAdapt tool [*Martin*, 2011]. Using PEAR [*J. Zhang et al*., 2014], forward and reverse sequenced fragments with overlapping sequence regions were merged, and the nucleotide sequence orientation was standardized. Low-quality sequences were filtered and trimmed by Trimmomatic [*Bolger et al.,* 2014], and chimeras were removed by Chimera.Slayer. Finally, the QIIME pipeline was used to cluster sequences into operational taxonomic units (OTUs) and to taxonomically assign them employing the Greengenes database with a cutoff value of 97% [*Caporaso et al.,* 2010]. Older taxonomic assignments for bacteria were corrected manually after *Rinke et al.* [2013] and *Nobu et al.* [2016]. OP9 and JS1 were renamed to *Atribacteria*, OD1 to *Parcubacteria*, and CD12 to *Aerophobetes*.

2.7. Statistical Analyses

$OTU_{0.03}$ with reads <0.1% of the total read counts per sample, $OTU_{0.03}$ not classified as bacteria or classified as chloroplasts, and absolute singletons were removed prior to statistical analysis. Absolute read counts were transformed to relative abundances in order to standardize the data and to account for different sequencing

depths. Variation in pore water and $OTU_{0.03}$ composition between samples and among pore water units, as well as correlations of the $OTU_{0.03}$ composition structure with pore water parameters, and determination of diversity were assessed using the Past 3.12 software [*Hammer et al.,* 2001]. Diversity indices and richness were calculated based on the mean relative abundance of all $OTU_{0.03}$ of duplicates. To visualize the grouping patterns of sediment samples based on pore water data, principal component analyses based on the Euclidean distance of standardized ($(x - \text{mean})/\text{stdev}$) pore water variables were used. Grouping patterns based on the $OTU_{0.03}$ composition of samples were determined by nonmetric multidimensional scaling (NMDS) based on the Bray-Curtis distance measure. To test whether pore water units and their communities, as well as the total communities of the two study sites, were significantly different, a nonparametric multivariate analysis of variance (MANOVA)/permutational MANOVA (PerMANOVA) was conducted [*Anderson*, 2001]. Mantel tests were used to study the relationship between pore water units and community structuring effects [*Mantel*, 1967].

Determination of the core community of $OTU_{0.03}$ in two different pore water units was performed using a custom R script. We filtered specialist $OTU_{0.03}$, which were present in all samples of one unit but not in the other.

2.8. Total Cell Counts

Fixation, sonication, and filtration of sediment were performed as previously described [*Llobet-Brossa et al.,* 1998]. In order to prevent lysis of the cells during the hybridization process, macromolecules and cytoskeletal structures were stabilized by fixation with formaldehyde. At the same time, the fixation makes the cell walls permeable. An amount of 0.5 g of sediment was fixed with 1.5 mL 4% paraformaldedhyde-phosphate-buffered saline (PBS; composed of 137 m*M* NaCl, 2.7 m*M* KCl, 15 m*M* Na_2HPO_4, and 1.7 m*M* KH_2PO_4 [pH 7.6 in water]) for 1 h at room temperature or at 4°C overnight. After incubation, the sediment was pelleted by centrifugation at 9600 *g* for 5 min, and the supernatant was discarded. The paraformaldehyde fixed samples were washed twice in freshly sterile filtered 1.5 mL PBS and stored in 1.5 mL of PBS/ethanol (1:1) at −20°C until further processing. The following sonication, according to *Ishii et al.* [2004], was performed to relieve cells attached to sediment particles. A volume of 200 μL of the fixed sample was diluted sixfold in PBS/ethanol (1:1), placed on ice, and treated by low intensity sonication with a Sonotrode MS73 probe (Sonopuls HD3100, Bandelin, Berlin, Germany) for 30 s at a setting of 1.5 s sonication pulses (on/off 0.5 s/1.0 s) and an amplitude of 20%. Sonication was repeated two times. After each sonication step, the sample was resuspended. Of the supernatant, 200 μL was transferred to a fresh tube and replaced by 200 μL of PBS/ethanol. The collected supernatant was chilled on ice for 2 min or stored at −20°C until further processing. The sonicated supernatant was diluted in PBS and filtered through a polycarbonate membrane filter. The filtration was performed by applying a vacuum and a pressure of around −5 mbar. Finally, the filters were air dried at room temperature and stored at −20°C until further processing [*Ishii et al.,* 2004].

Total cell counts were determined by SYBR Green I. Filters were placed on a glass slide, mounted with 3 μL of SBYR Green I staining solution (1 volume of 1:40 SYBR Green I, 1 volume of 0.1% *p*-phenylenediamine, and 1 volume of 4:1 Citifluor/Vecta Shield) and covered with a cover slip [*Kallmeyer et al.,* 2008]. Fluorescence microscopy was performed with a Leica DM2000 fluorescence microscope using the filter cube FI/RH for SYBR Green I.

3. Results

3.1. Pore Water Chemistry

According to the PCA of C2 and BK2 (Figure 1), variance between the samples on the horizontal axis (PC1) is explained by the seawater influence represented by salinity, conductivity, and most of the ion concentrations (Br^-, Cl^-, Na^+, Mg^{2+}), with nonsaline sediments to the left and saline sediments to the right side. In each plot, different clusters contained samples of consecutive depth, thus defining pore water units in the sediment. Pore water unit I (PW I) represented samples in the upper meters of both cores and is characterized by elevated salinity, conductivity, and ion concentrations. Pore water unit II (PW II) represented samples located below PW I. These sediments showed a rapid decline of cations, anions, salinity, and conductivity. The parameters mentioned before were lower than in PW I but still elevated in comparison to the underlying samples,

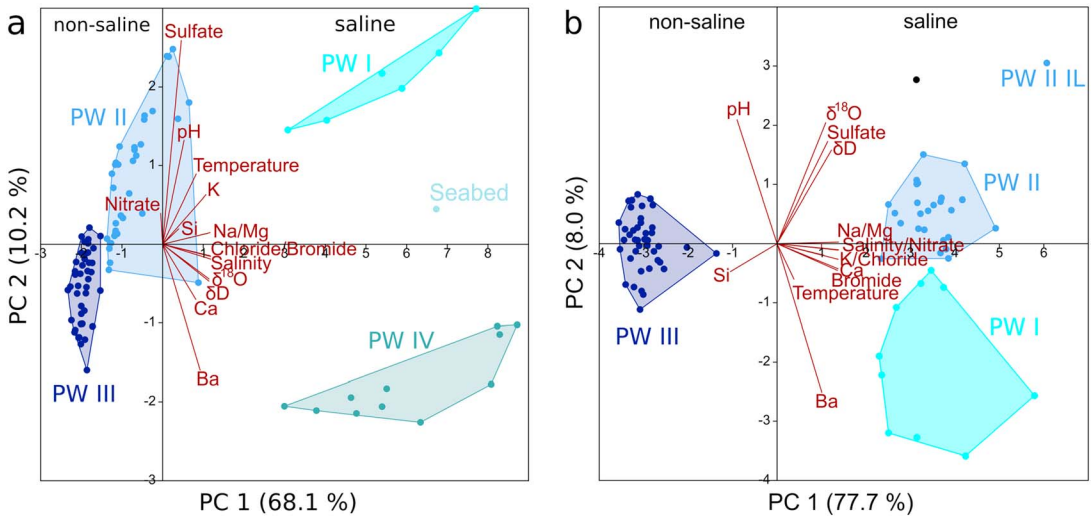

Figure 1. Principal component analyses show the variation of sediment samples based on standardized pore water and temperature data (Euclidean distance). Pore water units (PW) were defined based on cluster analysis and are represented by different colors. The percentage of variation between samples described by principal components 1 and 2 (PC 1 and 2) is indicated on the axes. (a) In total, PC 1 and PC 2 explained 78.3% of the variance between samples of C2 (inundated ~2500 years ago). (b) PC 1 and PC 2 explained 85.7% of variance between samples of BK2 (inundated 540 years ago). Environmental variables are projected as dark red vectors.

which represented the pore water unit III (PW III). These were not influenced by seawater: salinity was less than 1 psu for most samples.

In C2, clusters of PW II and PW III are not very distinct from each other (Figure 1a), as the influence of the saline water (concentration of ions, etc.) decreased gradually with depth, leading to a smooth transition from one unit to the other. Furthermore, an additional cluster formed (PW IV), representing samples in the unfrozen sediments below PW III, located deepest in the core. Although clustering apart from PW I on the vertical axis, parameters were comparable (high salinity and ion concentrations). Pore water stable isotope signatures in PW I and IV laid in the range of −9 to −20‰ ($\delta^{18}O$) and −75 to −150‰ (δD), where increasing marine influence was shown by a tendency toward heavier values. PW III had values consistent with a glacial origin of pore water, with values from −30 to −20‰ ($\delta^{18}O$) and −150 to −230‰ (δD). A one-way PerMANOVA still revealed that the variance between each of the clusters was significantly higher than within single clusters ($p = 0.0001$, supporting information Table S5). One single sample was located between the clusters of PW I and PW IV (Figure 1a), representing the uppermost centimeters of sediment, namely the seabed.

In contrast to C2, the separation of PW II and PW III in BK2 was very clear (Figure 1b). Salinity, conductivity, and the concentrations of all ions showed a sudden drop at the depth of 28.75 m bsl, the same depth at which the ice-bonded permafrost table occurred. The seawater penetration abruptly stopped at this depth, leaving the underlying sediments (PW III) unaffected. In BK2, PW I and PW II clustered close together as both were comparably strongly influenced by seawater. Variations in pore water stable isotope signature for the Buor Khaya borehole were discussed in *Overduin et al.* [2015] and suggest a terrestrial cold climate origin not yet affected by the infiltration of seawater in PW III. Together with pH and barium and sulfate concentrations, isotopes were important in differentiating PW I from PW II sediments in BK2. However, the difference between all three clusters determined by one-way PerMANOVA was significant ($p = 0.0001$, supporting information Table S6). Two samples were located apart from any cluster. One of them originated from the first few centimeters of sediment recovered (6 m bsl, black). However, the most deviant sample (PW II IL) originated from 12.35 m bsl depth, most closely located to PW II.

Analyses of samples from both cores in one principal component analysis (supporting information Figure S2) revealed that the PW III of both cores and PW II of C2 clustered together. Furthermore, the PW I of both cores, PW IV in C2, and PW II in BK2 clustered on the opposite site of the plot with increased influence of the salt water. PW II of C2 scattered between the PW I/PW II and PW III with most of the samples clustering close to PW III. In terms of pore water parameters, one-way PerMANOVA revealed no significant difference between both sediment cores ($p = 0.9999$; $F = -0.0005$).

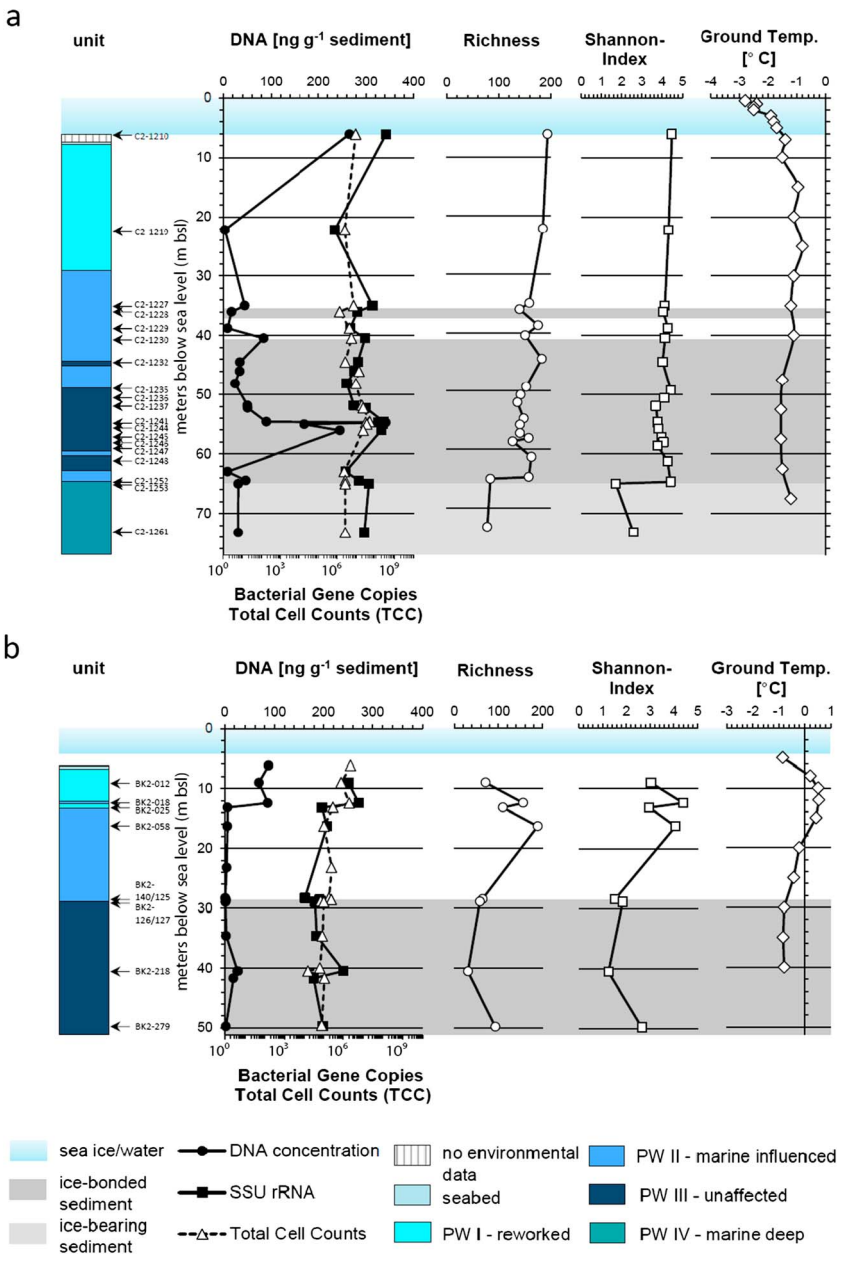

Figure 2. Sediment characteristics: (left to right) pore water units, depth of samples chosen for sequencing, DNA concentration (filled dots), bacterial 16S rRNA gene copy number (filled squares) and total cell counts (TCC, triangles) per gram sediment wet weight, richness (no. of $OTU_{0.03}$, dots), Shannon Index (diversity, squares), and ground temperature (diamond) of (a) C2 (inundated ~2500 years ago) and (b) BK2 (inundated 540 years ago). Sea ice/water thickness is indicated at the top of the figures; ice-bonded permafrost is shown in the graphs.

3.2. Stratification of Pore Water Units

Grouping the samples according to the previously shown clusters resulted in a clear separation of the PW I and II in the PCA, which was reflected in the stratigraphy of C2 (Figure 2a). PW I reached down to a depth of 29 m without interruption, whereas PW II and III showed some alternating layering effects in some depths. PW II reached down to a depth of 48.8 m bsl and was interrupted by PW III at between 44.7 and 45.2 m bsl. The largest zone of PW III extended to more than 10 m from 48.8 to 62.3 m bsl with an interlayer of PW II at 60.5 m bsl. Below PW III, again a layer of PW II occurred and reached down to a depth of 64.5 m bsl. This was followed by sediments which were similar to the PW I, namely pore water unit IV (PW IV).

The PW I in BK2 reached down to a depth of 13.65 m bsl (Figure 2b). An interlayer at the depth of 12.35 m bsl, resulting from the sample clustering far apart of any cluster (PW II IL in Figure 1b), divided this unit into upper and lower parts. PW II reached down to a depth of 28.75 m bsl. Frozen sediment below the permafrost table, unaffected of marine waters, formed the PW III.

3.3. Microbial Abundance in Submarine Permafrost

DNA concentrations of C2 are illustrated in Figure 2a and showed a high value of 265.2 ng g^{-1} in the upper centimeters right below the seafloor. A small DNA peak of 84.3 ng g^{-1} was found in the PW II sediment at a depth of 40.4 m bsl. But the highest DNA concentrations with maxima between 89.9 and 341.5 ng g^{-1} were found at the depth interval of 54.6 to 56.1 m bsl in the frozen PW III. The depth profile of the microbial abundance showed the same trend. The uppermost sample just below the seafloor revealed high numbers of 9.2×10^6 cells and 3.5×10^8 gene copies, but total cell counts and bacterial 16S rRNA gene abundance peaked again between 54.6 to 56.1 m bsl, with ~5×10^7 cells g^{-1} and 2.7×10^8 gene copies.

In comparison, BK2 (Figure 2b) exhibited three to four times lower DNA concentrations than C2 (Figure 2a). Cell counts were 20 to 70 times lower, and the abundance of the bacterial 16S rRNA gene was even 50 to 250 times lower than in C2. In contrast to C2, the highest biomass here was found in the upper meters of the sediment core. In PW I and the thin interlayer of PW II, DNA concentrations reached values of 68.3 to 87.9 ng g^{-1}. The lower part of PW II was characterized by very low values not exceeding 6 ng g^{-1}. Lowest DNA concentrations were obtained at the transition of frozen to unfrozen sediment with minimum values of 1.0 ng g^{-1} right above the ice-bonded permafrost table (IBPT). In the unaffected frozen unit (PW III), DNA concentrations peaked at a depth of 40.5 m bsl with 25.9 ng g^{-1}. Depth profiles of both bacterial gene copies and total cell counts were similar. Highest values in BK2 were obtained in the PW I and its interlayer with up to 2.4×10^6 cells and 6.2×10^6 gene copies. The second highest value of 1.1×10^6 gene copies was found in the ice-bonded part at a depth of around 40.5 m bsl, but generally cell counts in BK2 decreased with depth.

3.4. Diversity

The richness and diversity of C2 (Figure 2a) were quite constant from the seabed to PW III, with the highest values in the marine sample and a slightly decreasing trend. Here mean $OTU_{0.03}$ numbers of duplicates ranged between 127 and 194, in contrast to $OTU_{0.03}$ numbers of 78 to 84 in PW IV (supporting information Table S7). Diversity indices behaved very similar (Shannon index 3.7 to 4.5; Simpson index >0.9 in PW I–III and Shannon index 1.7 to 2.6; Simpson index 0.5 to 0.8 in PW IV).

In BK2, values of the Shannon index and the richness of $OTU_{0.03}$ showed a similar trend (Figure 2b). Both were highest in the unfrozen part (PW I and II) of BK2 and lowest in the permafrost unit PW III. Mean $OTU_{0.03}$ numbers of duplicates ranged between 31 and 189 per sample (supporting information Table S7). A decrease could be observed right above the phase boundary and in the ice-bonded PW III. Those depths were highly dominated by a few taxa.

3.5. Structure of the Bacterial Community

Using the relative abundances of $OTU_{0.03}$ and the Bray-Curtis distance measure, ordination plots were created (NMDS). The NMDS ordination of all samples from both cores showed some level of clustering of the bacterial communities in accordance with the separation by regional properties and environmental factors (supporting information Figure S3). Bacterial communities of both study sites formed two significant clusters (supporting information Table S8).

Individually, C2 exhibited distinct microbial communities according to the pore water units (Figure 3a). The NMDS plot showed an arrangement of the communities according to the depth location of pore water units. The community of the deep PW II was located between the PW II and PW III clusters showing the similarity to both of them. The microbial communities on the $OTU_{0.03}$ level differed significantly between the units (supporting information Table S9). A Mantel test with the total community and pore water data, including temperature, revealed a significant correlation ($p = 0.001$, correlation $R = 0.46$). Mantel tests with the total community and single pore water parameters at the corresponding depths showed that there was no correlation with calcium, silicon, and nitrate, and only a weak correlation with sulfate ($R < 0.25$; supporting information Table S10).

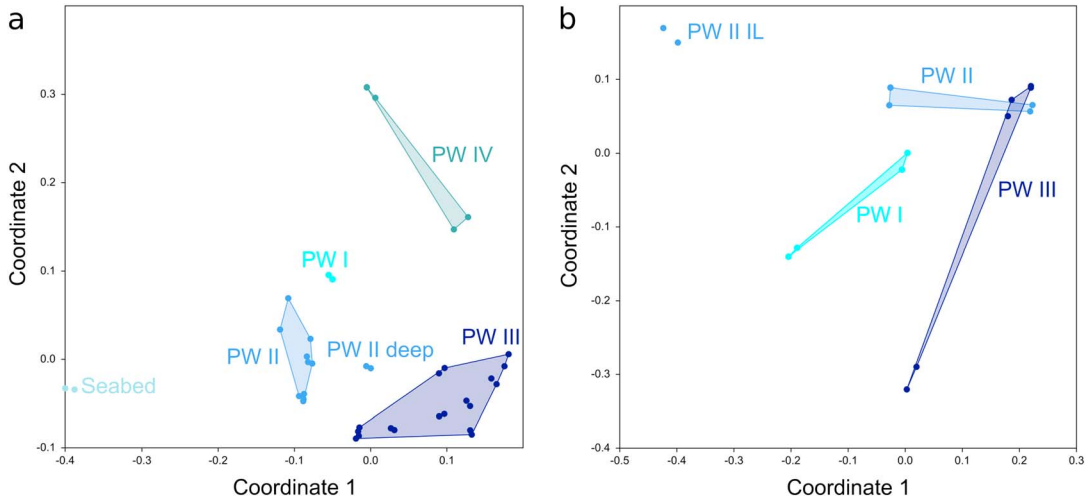

Figure 3. Nonmetrical multidimensional scaling of the microbial community structure based on relative abundances of $OTU_{0.03}$ (Bray-Curtis dissimilarity). Colors represent the pore water units from which the $OTU_{0.03}$ originate. (a) NMDS of bacterial communities found in C2 (inundated ~2500 years ago). The seabed is not defined by pore water but by the shallow depth location of the sample. Stress: 0.12. (b) NMDS of bacterial communities found in BK2 (inundated 540 years ago). PW II IL means the interlayer of pore water unit II within PW I. Stress: 0.07.

In BK2, we did not observe bacterial community structures that were specific for any pore water unit (Figure 3b). In addition to the corresponding pore water data, the bacterial community of the sample at 12.35 m depth (PW II IL) differed from the others. Grouping the samples according to the pore water units showed an overall significant difference between those groups, but not when considered pairwise (supporting information Table S11). Furthermore, there was no correlation of the overall community composition of BK2 to pore water parameters (p = 0.357, R = 0.07).

The most abundant phyla of C2 and BK2 on the order level are shown in Figures 4a and 4b and supporting information Tables S12 and S13. In BK2, 90 orders were identified (supporting information Table S14), but only 17 had >3% abundance. The bacterial community of C2 consisted of 138 identified orders with 34 exceeding a relative abundance of 3%, twice the number of BK2.

The composition and distribution of the most frequent orders (>3%) of both sediment cores showed few similarities. Only *Clostridiales* were found to be abundant in several units of both cores. *Atribacteria* SB-45 was abundant in units with elevated salt concentrations (PW IV in C2 and PW I and II in BK2), *Burkholderiales* in units with low salinity, and *Rhizobiales* throughout all PW units (Figure 4).

In C2, no clear marine or terrestrial community was observed, except for the uppermost sample of C2 representing the seabed, because many of the observed taxonomic groups can be found in both marine and terrestrial environments. The seabed was characterized by many marine-related orders which were unique for that horizon, such as *Pirellulales* and orders of the *Deltaproteobacteria* (*Desulfobacterales*, MBNT15, *Myxococcales*) and *Gammaproteobacteria* (*Chromatiales*, *Thiotrichales*, *Marinicellales*). In regard to the dominant orders, PW I to PW III showed a quite similar community composition. Community characteristics of PW units and differences between them are described in the following. PW I mainly contained groups that could be found elsewhere in PW II or PW III sediments (*Acidimicrobiales*, *Actinomycetales*, *Gaiellales*, *Solirubrobacterales*, *Chloroflexi* Gitt-GS-136, *Gemmatimonadetes* Gemm-1, *Rhizobiales*, *Sphingomonadales*) and that were mostly absent from the shallowest and deepest layers (seabed and PW IV). Abundant groups, such as *Actinomycetales* and Gitt-GS-136, were found in all PW I to PW III. Both underwent a shift on family level from PW II to PW III. *Actinomycetales* in PW II were dominated by *Nocardioidiaceae*, whereas *Intrasporangiaceae* and *Actinotalea* dominated in PW III. Further, *Chloroflexi* Gitt-GS-136 was abundant in PW II, while in PW III, *Chloroflexi* Ellin6529 was more abundant. Besides *Actinomycetales* and *Chloroflexi*, *Clostridiales* was among the most abundant orders in PW III. In addition, PW III contained numerous taxa that were unique for this pore water unit (for example, *Acidobacteria* iii1–15, *Gaiellales*, *Bacteriodales*, or *Gemmatimonadetes* N1423WL). The deepest unit PW IV was highly dominated by *Clostridiales* and SB-45 of the phylum *Atribacteria*. Due to the high dominance of *Clostridia*, there were only two other taxa

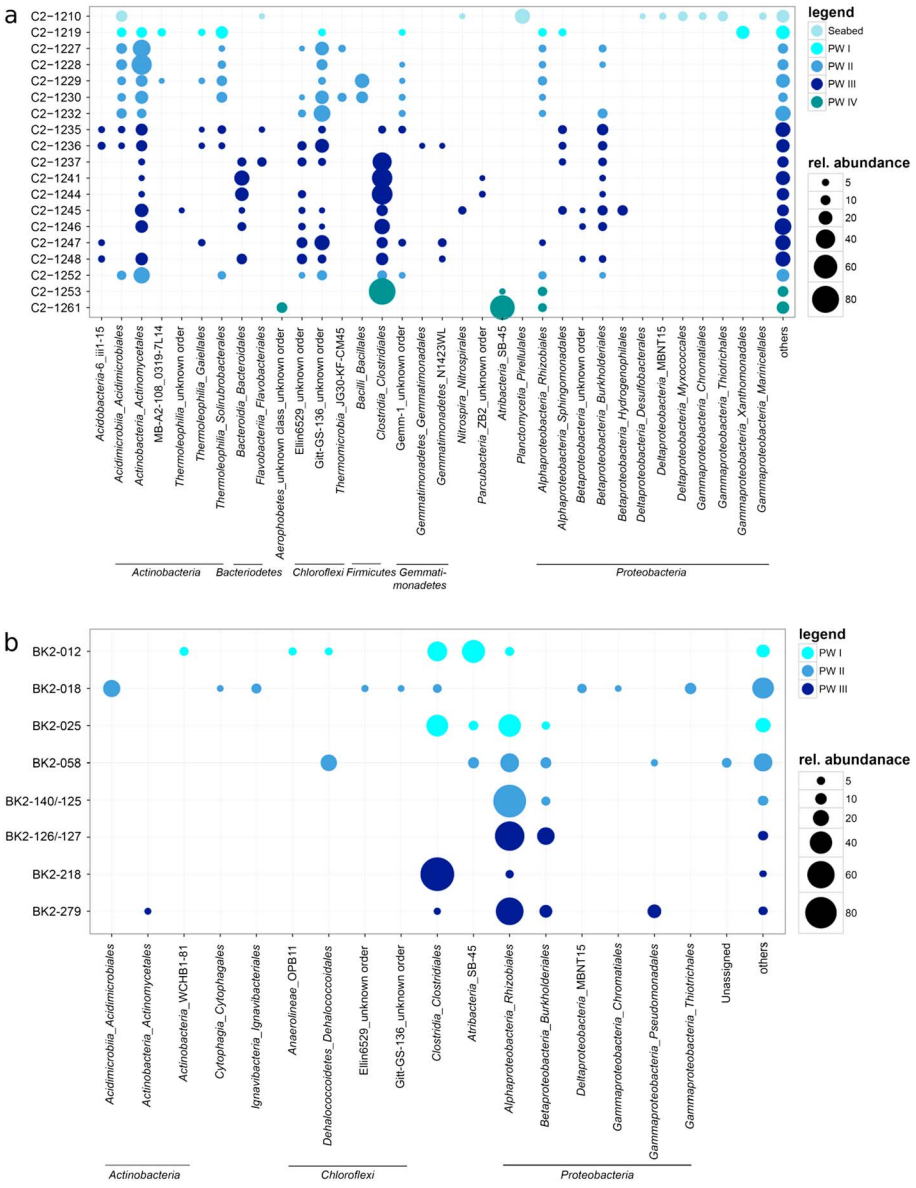

Figure 4. Relative abundance of bacterial orders of samples from (a) C2 (inundated ~2500 years ago) and (b) BK2 (inundated 540 years ago). Orders with an abundance of more than 3% are shown. The remaining orders are categorized as "others." Colors indicate the pore water unit.

(*Aerophobetes* and *Rhizobiales*) with a sequence abundance above 3%. In general, PW IV comprised less taxa, reflected in a lower diversity and richness compared to the other units (see supporting information Table S7).

In BK2, a few taxa such as *Clostridiales* and *Rhizobiales* were highly abundant especially within PW III and right above the permafrost table. The bacterial community of the sample BK2-018 was very different from that of all other samples (Figure 4b) coinciding with the pore water data (Figure 1b, PW II IL) and the $OTU_{0.03}$ data (Figure 3b, PW II IL). Except for *Clostridiales*, all other taxa (for example *Acidimicrobiales*, *Cytophagales*, *Ignavibacteriales*, *Chromatiales*, and *Thiotrichales*) were only observed in BK2-018. Core groups of BK2 were *Clostridiales*, *Rhizobiales*, and *Burkholderiales* and were found in all three pore water units of BK2.

In addition to the general community composition, we investigated the core communities of PW II and PW III in C2 (supporting information Table S15). We excluded PW I due to the low sample number. Given the overall low sample number in BK2, a determination of the core communities was not reasonable. The core community of PW II in C2 was much more diverse than that of PW III, counting 28 $OTU_{0.03}$. In contrast, the

community of PW III in C2 contained only eight shared $OTU_{0.03}$. Taxa such as *Acidimicrobia*, *Actinobacteria*, and *Thermoleophilia* were represented by several $OTU_{0.03}$ in PW II but completely absent in the core community of PW III. In contrast to the seabed, a clear marine origin of PW II taxa was not evident. Some taxa such as *Acidimicrobiales* (*Acidimicrobia*), *Nocardioidaceae* and *Geodermatophilaceae* (*Actinomycetales*), and *Hyphomicrobiaceae* (*Rhizobiales*) were, however, reported to be successful in marine environments [*Yi and Chun*, 2004; *Lee and Kim*, 2007; *Normand et al.,* 2014; *Oren and Xu*, 2014; *D. F. Zhang et al*., 2014; *Mizuno et al.,* 2015].

4. Discussion

Bacterial communities in two submarine permafrost settings from the East Siberian Arctic Shelf (BK2 and C2) were exposed to permafrost warming and thaw and the infiltration of seawater by inundation for about 540 and 2500 years, respectively. The inundation period was thereby based on recent rates of coastal retreat. Although the rate at which the sea transgresses over land is determined by many different factors, the degradation of permafrost in the nearshore zone is at least partially controlled by the coastal erosion rates [*Are*, 2003; *Overduin et al.,* 2016]. Due to a high mean annual coastal erosion rate of 4.5 m yr^{-1} over the past decades at the C2 site [*Grigoriev*, 2008], we assume an initially rapid submergence relative to BK2. The more rapid erosion at the C2 site leads to shorter times for seawater penetration for a particular distance from the coast, all other factors being equal. In contrast, the comparably low mean annual coastal erosion rate over the past decades of 1.4 m yr^{-1} means that inundation occurred more slowly at BK2. The proximity of BK2 to the coast and the shallower water suggests that seasonal changes in salinity and temperature are probably still large due to this proximity and that wave action will penetrate more deeply into the sediment [*Overduin et al.,* 2015]. The marine influence, characterized by a constant salinity in the unfrozen sediment of BK2, extended down to the ice-bonded permafrost table, suggesting convective downward transport of salt [*Overduin et al.,* 2015]. The coupling of heat with convective transport [*Osterkamp*, 2001] and higher terrestrial permafrost and geothermal heat fluxes in this region [*Nicolsky et al.,* 2012] likely also explain high sediment temperatures (−0.8 to 0.5°C) of BK2.

Although both coring sites belong to the ice-rich syngenetic permafrost deposits called Yedoma or Ice Complex [*Schirrmeister et al.,* 2008, 2016; *Grosse et al.,* 2013], C2 is located 250 km westward and 550 northward of BK2. Despite their spatial separation and differing glacial sediment source regions, the sub-Yedoma terrestrial sandy sediment at both sites was deposited in similar local fluvial-alluvial environments with intermittent organic layers of woody and fibrous detritus [*Winterfeld et al.,* 2011; *Overduin et al.,* 2015]. The portions of the two cores undergoing submarine degradation have similar ages [*Winterfeld et al.,* 2011; *Schirrmeister et al.,* 2016]. Permafrost at the C2 site has a temperature close to −12°C at the damping depth for annual temperature fluctuations; at BK2, the temperature is similar though closer to −10°C, probably due to differences in regional climate. There were similarities between how pore water chemistry varied over depth in both cores, which reflected similar stages of permafrost degradation. PW III represents ice-bonded and warmed permafrost that was unaffected by the infiltration of seawater. PW I and II were found in permafrost of terrestrial origin that had been influenced by seawater. PW IV was only observed in one of the cores, where drilling penetrated through the frozen permafrost into a partially frozen marine layer. *Winterfeld et al.* [2011] suggested that the corresponding sediment layer was Eemian and marine in origin. The similarity of pore water units at the two sites suggests that they are characteristic of submarine permafrost. They can be partly explained by postdepositional and posttransgression processes: wave and ice turbation of the seabed (PW I) and infiltration of saline seawater into the sediment (PW II). In addition to warming of the sediment by the overlying seawater, these processes contribute to thawing of permafrost below the seabed after inundation. In C2, for example, PCA strongly suggests that seawater infiltrates into ice-bonded permafrost before thawing is complete. Higher solute concentrations decrease the temperature of freezing of the pore water and increase the liquid water content of the sediment [*Overduin et al.,* 2008]. Since freezing affects the volume of the habitable space in the sediment and the concentration of solutes in that habitable space, depending on temperature and salinity, freezing is an important control on microbial activity. Determination of the in situ ice and liquid water content in the sediment at the time of sampling or during the period of warming following inundation is difficult for samples at or close to freezing temperature. Based on the measured pore water salinities, pore water solutions had freezing points of between −1.76 and −0.6°C for PW I and IV and −0.9 and 0°C for PW II and III. The almost isothermal temperature profile in

supporting information Table S1, for example, showed sediment at or near the freezing point, especially in PW IV. Permafrost dynamics and pore water composition in particular thus expand the bacterial habitat and have the potential to influence bacterial community composition.

The stratification of bacterial subcommunities at C2 (Figure 3a) coincides with changes in the bacterial community composition (Figure 4a). For example, the shallowest sample of C2, a few centimeters below the seafloor, harbored the highest number of unique phyla and predominantly those typical for marine conditions such as *Pirellulales*, *Desulfobacterales*, *Thiotrichales*, and *Marinicellales* [*Wang et al.,* 2012; *Campbell and Kirchman*, 2012]. The bacterial community composition of this layer thus shows a marine origin, so that we refer to it as the seabed. The underlying subcommunities of PW I and II lack an imprint of clearly marine taxa despite seawater infiltration and even though parameters such as salinity and stable water isotopes largely serve to explain their community patterns (supporting information Table S10). At the same time, they have evolved into subcommunities significantly different from those of the unaffected permafrost unit PW III (supporting information Table S9). The separation into individual subcommunities of PW II and III is further manifested through different core groups of both layers (supporting information Table S15). So, although the bacterial community composition has changed in response to seawater infiltration, it reflects the bacterial assemblages of terrestrial permafrost even after centuries to millennia of exposure to submarine conditions. In C2, bacterial communities can consequently be classified as belonging to terrestrial permafrost, marine-affected permafrost, reworked permafrost sediments, or seabed. Continuing permafrost thaw will eventually lead to the complete loss of the original permafrost bacterial assemblages. They will probably shift to new assemblages like those of PW II but remain distinct in their composition from bacterial communities at the seabed. In contrast to C2, no significant correlation between community and environmental data along the BK2 core was observed, meaning that an assignment of bacterial communities consistent with pore water units was not possible. The statistical lack of significance may have been the result of low biomass in BK2.

With total cell counts of 10^3–10^7 cells g^{-1} sediment, the microbial abundances of both submarine permafrost cores were within the range of cell counts found in terrestrial long-term cryogenic formations such as frozen ground and buried soils [*Gilichinsky,* 2008]. Cell numbers of C2 were comparable with microbial abundances from subseafloor sediments (10^6–10^7 cells mL^{-1} sediment) [*Parkes et al.,* 2014]. The depth profiles of total DNA concentration, bacterial gene copy numbers, and total cell counts in both cores followed a similar trend. Still, in C2 the abundance of the bacterial 16S rRNA gene often exceeded that of the total cell counts by at least an order of magnitude (supporting information Tables S16 and S17). This cannot be solely due to multiple 16S rRNA gene copies per cell [*Schmidt*, 1998] but reflects the long-term preservation of extracellular DNA (up to 400,000 years) due to low temperature conditions in permafrost [*Stokstad,* 2003; *Willerslev et al.,* 2004]. A large proportion of external DNA has frequently been observed in marine sediments as well [*Corinaldesi et al.,* 2005; *Alawi et al.,* 2014; *Kirkpatrick et al.,* 2016]. Future cell separation approaches will shed light on the extent and distribution of external DNA versus DNA of intact cells. In subseafloor sediments, the microbial abundance usually shows an exponential decrease with depth [*Kallmeyer et al.,* 2012]. In C2, however, maximum microbial abundances, bacterial gene copy numbers, and DNA concentrations occurred in the unaffected permafrost unit, which confirms that even in frozen sediments microbial cells can be conserved and survive within thin brine veins [*Steven et al.,* 2007; *Wagner et al.,* 2007; *Bischoff et al.,* 2013]. C2 also exhibited a quite constant diversity and richness in all pore water units except for PW IV. The diversity of this submarine permafrost site is thereby comparable with the permafrost active layer and permafrost thaw ponds [*Liebner et al.,* 2008; *Crevecoeur et al.,* 2015], though lower than in marine and deep-sea hydrothermal sediments [*Wang et al.,* 2012; *Cerqueira et al.,* 2015]. Recalling the clear stratification of bacterial assemblages according to the degree of marine influence, C2 displays thus a very unusual subseafloor habitat where permafrost table depth, stage of permafrost degradation, and time of inundation are constraints for the abundance and structure of bacteria and where permafrost is a bottom-up source for subseafloor life. "Bottom-up" refers in this case to its vertical position and the fact that, due to permafrost thaw, it is being continuously released at the lower boundary of the thawed sediment layer. Since C2 can be considered representative for submarine permafrost after millennia of exposure to submarine conditions, its unique features as a subsurface habitat are likely applicable to large areas of the Siberian Arctic Shelf.

The origin and development of bacterial community structure and diversity differ between the two submarine permafrost cores. β-diversity, the variation in community composition, increases with distance and

when local environmental conditions differ [*Lindström and Langenheder*, 2012]. Given that the terrestrial sediment at both sites was deposited in similar local fluvial-alluvial environments, we assign the high β-diversity of the bacterial communities to the large spatial distance and different glacial sediment source regions. Not even the infiltration of seawater into the units PW I and II resulted in similar bacterial community structure of C2 and BK2 (supporting information Figure S3 and Table S8) even though dispersal, i.e., the movement of an individual taxon from one location to another by passive or active mechanisms [*Hanson et al.,* 2012], through seawater should be high [*Lindström and Langenheder*, 2012]. For example, abundant taxa of PW II in BK2 were *Rhizobiales* and *Burkholederiales*, whereas PW II in C2 harbored predominantly *Acidimicrobiales*, *Actinomycetales*, and *Chloroflexi* Gitt-GS-136. The heterogeneity of bacterial communities in shelf sediments of the Laptev Sea is in line with a substantial β-diversity of bacterial communities in deep marine subsurface sediments from different continental margin sites in the Pacific Ocean [*Fry et al.,* 2008]. A large β-diversity even in sediment layers influenced by seawater for decades and hundreds of years could reflect (i) that marine bacterial taxa did not establish in the new location of formerly terrestrial sediment, (ii) the movement of seawater through the sediment matrix is too slow, or (iii) the movement of seawater through the sediment matrix occurs at very different rates in C2 compared to BK2. Our results indeed show that sediments of terrestrial origin in C2 are less influenced by marine inundation than sediments in BK2. The more gradual transition between PW II and PW III (Figure 1a) in C2, compared to BK2, indicates that the penetration of seawater into the sediment takes place more slowly in C2. This can be due to different seabed conditions caused by wave and sea ice action, which drive the diffusive penetration into the seabed, and/or distinct sediment column properties that affect the penetration rate [*Ulyantsev et al.,* 2016]. As a consequence of the relatively deep water column and the low sea ice thickness, seasonal changes in seabed temperature and salinity were likely lower in amplitude at the C2 site. Still, bottom water salinity in the western part of the Laptev Sea is higher than in the central Laptev Sea, which is influenced by fluvial discharge [*Schirrmeister*, 2007; *Charkin et al.,* 2011; *Günther et al.,* 2013]. The concentration profile in C2 [*Winterfeld et al.,* 2011] suggests a predominantly diffusive transport of dissolved constituents of the pore water through the sediment column, whereas the BK2 profile suggests either more rapid diffusion and/or advective transport [*Osterkamp*, 2001].

C2 furthermore appears to host bacterial communities that have been stimulated by warming and started to proliferate, an assumption that was made before in the context with submarine permafrost [*Koch et al.,* 2009] and that is generally associated with the development of microbes in thawing permafrost [*Graham et al.,* 2012; *Schuur et al.,* 2015]. Thereby, stimulation of the microbes may be facilitated by a rising water content in warming permafrost [*Overduin et al.,* 2008]. This is supported by highest total cell counts, DNA concentrations, and bacterial gene copy numbers of all units in the ice-bonded unaffected permafrost unit of C2, when neglecting the seabed sample. We cannot, however, rule out that cell numbers were high before transgression. The drop in microbial abundance between the unaffected permafrost unit (PW III) and the terrestrial units that are marine-influenced (PW I and II) further indicate that in C2 the microbial community was disturbed by seawater infiltration. This would be in line with observed decreases in soil microbial abundance after exposure to elevated salt concentrations [*Rietz and Haynes,* 2003]. In BK2, microbial cell numbers decrease with depth which is typical for subseafloor habitats. In addition, the microbial data along BK2, for example, the lowest microbial abundance in the seawater-unaffected permafrost sediments, do not show any indication for proliferation due to warming. The ice-bonded permafrost is still characterized by subzero temperatures, an environment where water activity, rates of nutrient exchange, and growth rates are low [*Rivkina et al.,* 2000]. Microorganisms must resist exposure to subzero temperatures for prolonged periods of time [*Wagner et al.,* 2007]. This is highly selective for cells and may be the reason for the small bacterial diversity and population size (10^4 cells g^{-1} sediment) in BK2. In addition, a high mean acetate concentration of 132.6 μM in the unaffected sediments (supporting information Figure S4) indicate that despite the temperature increase, bacterial activity and growth in the permafrost unit were not yet stimulated. In fact, three orders of magnitude less microbial cells in PW III of BK2 compared to C2 suggest that the reaction of the permafrost bacterial community in BK2 to inundation is more strongly determined by disturbance than by the beneficial increase in temperature. As a corollary, this would suggest that bacterial communities in C2 reflect a later stage in the reaction of permafrost bacterial communities to marine transgression of permafrost.

5. Conclusions

This study highlights that submarine permafrost is a suitable natural laboratory for studying the response of permafrost bacterial communities both to temperature and salinity increase on geological timescales. It shows that concentrations and stable isotopes of pore water solutes can be used to distinguish sediments affected by reworking in the marine environment from the terrestrial permafrost thawed in situ beneath the seabed. Further, we show that seawater infiltrates into frozen ice-bonded permafrost before thawing is complete. The effect of these processes is also reflected in the bacterial communities found in thawed and frozen submarine permafrost. Submarine permafrost originates as terrestrial permafrost but is warmer and has more saline pore water as a result of inundation by seawater. These differences change bacterial community structure, abundance, and diversity, but the communities themselves remain terrestrial. The exposure to warming and increasing pore water salinity is a disturbance that probably results in a decrease of the community size followed by increasing proliferation on a timescale of millennia. Further work is needed to clarify whether differences in the community size and structure are a result of different inundation processes or spatial differences and whether microbes in unaffected sediments exposed to warming are actively proliferating.

Acknowledgments

Sequences of the submarine permafrost communities presented in this work were deposited at the NCBI Sequence Read Archive (SRA) with the Project number BioProject ID# PRJNA352907. Bacterial 16S rRNA gene sequences have the accession numbers SRR5184420-SRR5184446 and are available from Genbank, EMBL, and DDBJ. Pore water data for the C2 and BK2 cores are available at https://doi.pangaea.de/10.1594/PANGAEA.873837. Coring was supported by the German Ministry for Education and Research, a Joint Russian German Research Group (HGF-JRG100) of the Helmholtz Association of German Research Centres, and by the EU's INTAS program. Susanne Liebner is grateful for the funding of the Helmholtz Young Investigators Group (grant VH-NG-919). Our thanks go to Anke Saborowski, Monique Thiele, Linda Mahler, Antje Eulenburg, Ute Bastian, and Katja Hockun for excellent laboratory support, André Friese for acetate and formate measurements, and Jens Kallmeyer for sharing his knowledge in the field of cell counts. We further thank Aleksandr Maslov (SB RAS, Melnikov Permafrost Institute, Yakutsk, Russia), who provided indispensable drilling expertise, and we thank Tiksi Hydrobase staff members Viktor Bayderin, Viktor Dobrobaba, Sergey Kamarin, Valery Kulikov, Dmitry Mashkov, Dmitry Melnichenko, Aleksandr Safin, and Aleksandr Shiyan for their field support.

References

Alawi, M., B. Schneider, and J. Kallmeyer (2014), A procedure for separate recovery of extra- and intracellular DNA from a single marine sediment sample, *J. Microbiol. Methods*, *104*, 36–42, doi:10.1016/j.mimet.2014.06.009.

Allison, S. D., and J. B. H. Martiny (2008), Colloquium paper: Resistance, resilience, and redundancy in microbial communities, *Proc. Natl. Acad. Sci. U.S.A.*, *105*(1), 11,512–11,519, doi:10.1073/pnas.0801925105.

Anderson, M. J. (2001), A new method for non parametric multivariate analysis of variance, *Austral Ecol.*, *26*(2001), 32–46, doi:10.1111/j.1442-9993.2001.01070.pp.x.

Are, F. (2003), Shoreface of the Arctic seas—A natural laboratory for subsea permafrost dynamics, in *Permafrost: Proceedings of the 8th International Conference on Permafrost*, pp. 27–32, Zurich.

Bischoff, J., K. Mangelsdorf, A. Gattinger, M. Schloter, A. N. Kurchatova, U. Herzschuh, and D. Wagner (2013), Response of methanogenic archaea to Late Pleistocene and Holocene climate changes in the Siberian Arctic, *Global Biogeochem. Cycles*, *27*, 305–317, doi:10.1029/2011GB004238.

Bolger, A. M., M. Lohse, and B. Usadel (2014), Trimmomatic: A flexible trimmer for Illumina sequence data, *Bioinformatics*, *30*(15), 2114–2120, doi:10.1093/bioinformatics/btu170.

Brown, J., O. J. Ferrians Jr., J. A. Heginbottom, and E. S. Melnikov (2002), *Circum-Arctic Map of Permafrost and Ground-Ice Conditions, Version 2*, Natl. Snow and Ice Data Cent, Boulder, Colo.

Campbell, B. B. J., and D. L. D. D. L. Kirchman (2012), Bacterial diversity, community structure and potential growth rates along an estuarine salinity gradient, *ISME J.*, *7*(1), 210–220, doi:10.1038/ismej.2012.93.

Caporaso, J. G., et al. (2010), QIIME allows analysis of high-throughput community sequencing data, *Nat. Publ. Gr.*, *7*(5), 335–336, doi:10.1038/nmeth0510-335.

Cerqueira, T., D. Pinho, C. Egas, H. Froufe, B. Altermark, C. Candeias, R. S. Santos, and R. Bettencourt (2015), Microbial diversity in deep-sea sediments from the Menez Gwen hydrothermal vent system of the Mid-Atlantic Ridge, *Mar. Genomics*, *24*, 343–355, doi:10.1016/j.margen.2015.09.001.

Charkin, A. N., O. V. Dudarev, I. P. Semiletov, A. V. Kruhmalev, J. E. Vonk, L. Sánchez-García, E. Karlsson, and O. Gustafsson (2011), Seasonal and interannual variability of sedimentation and organic matter distribution in the Buor-Khaya Gulf: The primary recipient of input from Lena River and coastal erosion in the southeast Laptev Sea, *Biogeosciences*, *8*(9), 2581–2594, doi:10.5194/bg-8-2581-2011.

Corinaldesi, C., R. Danovaro, D. Anno, and A. D. Anno (2005), Simultaneous recovery of extracellular and intracellular DNA suitable for molecular studies from marine sediments, *Society*, *71*(1), 46–50, doi:10.1128/AEM.71.1.46.

Crevecoeur, S., W. F. Vincent, J. Comte, and C. Lovejoy (2015), Bacterial community structure across environmental gradients in permafrost thaw ponds: Methanotroph-rich ecosystems, *Front. Microbiol.*, *6*, 1–15, doi:10.3389/fmicb.2015.00192.

Fritz, M., J. E. Vonk, and H. Lantuit (2017), Collapsing Arctic coastlines, *Nat. Clim. Change*, *7*(1), 6–7, doi:10.1038/nclimate3188.

Fry, J. C., R. J. Parkes, B. A. Cragg, A. J. Weightman, and G. Webster (2008), Prokaryotic biodiversity and activity in the deep subseafloor biosphere, *FEMS Microbiol. Ecol.*, *66*(2), 181–196, doi:10.1111/j.1574-6941.2008.00566.x.

Galinski, E. A. (1995), Osmoadaptation in bacteria, *Adv. Microb. Physiol.*, *37*, 273–328, doi:10.1016/S0065-2911(08)60148-4.

Gilichinsky, D. (2008), *Psychrophiles: From Biodiversity to Biotechnology*, edited by R. Margesin et al., pp. 83–102, Springer Science & Business Media, Berlin, Germany.

Graham, D. E., et al. (2012), Microbes in thawing permafrost: The unknown variable in the climate change equation, *ISME J.*, *6*(4), 709–712, doi:10.1038/ismej.2011.163.

Grigoriev, M. N. (2008), *Kriomorphogenez i litodinamika pribrezhno-shelfovoi zony morei Vostochnoi Sibiri (Cryomorphogenesis and Lithodynamics of the East Siberian Near-Shore Shelf Zone) [in Russian]*, 315 pp., Russian Academy of Sciences, Siberian Branch, Yakutsk.

Grosse, G., J. Robinson, R. Bryant, M. D. Taylor, W. Harper, A. De Masi, A. Kyker-Snowman, E. Veremeeva, L. Schirrmeister, and J. Harden (2013), Distribution of late Pleistocene ice-rich syngenetic permafrost of the Yedoma Suite in east and central Siberia, Russia, *Geol. Surv. Open File Rep.*, 2013–1078, 37 pp.

Günther, F., P. P. Overduin, A. V. Sandakov, G. Grosse, and M. N. Grigoriev (2012), Thermo-erosion along the Yedoma Coast of the Buor Khaya Peninsula, Laptev Sea, East Siberia, *Tenth Int. Conf. Permafr.*, *2*, 137–142.

Günther, F., P. P. Overduin, A. S. Makarov, and M. N. Grigoriev (2013), Russian-German Cooperation System Laptev Sea: The Expeditions Laptev Sea—Mamontov Klyk 2011 & Buor Khaya 2012, in *Berichte zur Polar- und Meeresforschung = Reports on Polar and Marine Research*, 113 pp.

Hammer, Ø., D. A. T. Harper, and P. D. Ryan (2001), Paleontological Statistics software: Package for education and data analysis, *Palaeontol. Electron.*, *4*(1), 1–9.

Hanson, C. A., J. A. Fuhrman, M. C. Horner-Devine, and J. B. H. Martiny (2012), Beyond biogeographic patterns: Processes shaping the microbial landscape, *Nat. Rev. Microbiol.*, *10*, 1–10, doi:10.1038/nrmicro2795.

Harrison, W. D., and T. E. Osterkamp (1982), Measurements of the electrical conductivity of interstitial water in subsea permafrost, in *Proceedings of the Fourth Canadian Permafrost Conference*, edited by H. M. French, pp. 229–237, National Research Council of Canada, Ottawa, Canada.

Herlemann, D. P., M. Labrenz, K. Jürgens, S. Bertilsson, J. J. Waniek, and A. F. Andersson (2011), Transitions in bacterial communities along the 2000 km salinity gradient of the Baltic Sea, *ISME J.*, *5*(10), 1571–1579, doi:10.1038/ismej.2011.41.

IPCC (2013), *Climate Change 2013: The Physical Science Basis. Contribution of Working Group I to the Fifth Assessment Report of the Intergovernmental Panel on Climate Change*, edited by T. F. Stocker et al., 1535 pp., 1535 pp., Cambridge Univ. Press, Cambridge, U. K., and New York.

Ishii, K., M. Mussmann, B. J. MacGregor, and R. Amann (2004), An improved fluorescence in situ hybridization protocol for the identification of bacteria and archaea in marine sediments, *FEMS Microbiol. Ecol.*, *50*(3), 203–212.

Jones, B. M., C. D. Arp, M. T. Jorgenson, K. M. Hinkel, J. A. Schmutz, and P. L. Flint (2009), Increase in the rate and uniformity of coastline erosion in Arctic Alaska, *Geophys. Res. Lett.*, *36*, L03503, doi:10.1029/2008GL036205.

Junker, R., M. N. Grigoriev, and N. Kaul (2008), Non-contact infrared temperature measurements in dry permafrost boreholes, *J. Geophys. Res.*, *113*, B04210, doi:10.1029/2007JB004946.

Kallmeyer, J., D. C. Smith, A. J. Spivack, and S. D'Hondt (2008), New cell extraction procedure applied to deep subsurface sediments, *Limnol. Oceanogr. Methods*, *6*, 236–245, doi:10.4319/lom.2008.6.236.

Kallmeyer, J., R. Pockalny, R. R. Adhikari, D. C. Smith, and S. D'Hondt (2012), Global distribution of microbial abundance and biomass in subseafloor sediment, *Proc. Natl. Acad. Sci. U.S.A.*, *109*, 16,213–16,216, doi:10.1073/pnas.1203849109.

Kirkpatrick, J. B., E. A. Walsh, and S. D'Hondt (2016), Fossil DNA persistence and decay in marine sediment over hundred-thousand-year to million-year time scales, *Geology*, *44*(8), 615–618, doi:10.1130/G37933.1.

Koch, K., C. Knoblauch, and D. Wagner (2009), Methanogenic community composition and anaerobic carbon turnover in submarine permafrost sediments of the Siberian Laptev Sea, *Environ. Microbiol.*, *11*(3), 657–668, doi:10.1111/j.1462-2920.2008.01836.x.

Lantuit, H., et al. (2012), The Arctic Coastal Dynamics Database: A new classification scheme and statistics on Arctic permafrost coastlines, *Estuaries Coasts*, *35*(2), 383–400, doi:10.1007/s12237-010-9362-6.

Lee, S. D., and S. J. Kim (2007), *Aeromicrobium tamlense* sp. nov., isolated from dried seaweed, *Int. J. Syst. Evol. Microbiol.*, *57*(2), 337–341, doi:10.1099/ijs.0.64442-0.

Liebner, S., J. Harder, and D. Wagner (2008), Bacterial diversity and community structure in polygonal tundra soils from Samoylov Island, Lena Delta, Siberia, *Int. Microbiol.*, *11*(3), 195–202.

Lindström, E. S., and S. Langenheder (2012), Local and regional factors influencing bacterial community assembly, *Environ. Microbiol. Rep.*, *4*(1), 1–9, doi:10.1111/j.1758-2229.2011.00257.x.

Llobet-Brossa, E., R. Rossello-Mora, and R. Amann (1998), Microbial community composition of Wadden Sea sediments as revealed by fluorescence in situ hybridization, *Appl. Environ. Microbiol.*, *64*(7), 2691–2696.

Mackelprang, R., M. P. Waldrop, K. M. DeAngelis, M. M. David, K. L. Chavarria, S. J. Blazewicz, E. M. Rubin, and J. K. Jansson (2011), Metagenomic analysis of a permafrost microbial community reveals a rapid response to thaw, *Nature*, *480*(7377), 368–371, doi:10.1038/nature10576.

Mantel, N. (1967), The detection of disease clustering and a generalized regression approach, *Cancer Res.*, *27*(1), 209–220.

Martin, M. (2011), Cutadapt removes adapter sequences from high-throughput sequencing reads, *EMBnet J.*, *17*(1), 10–12, doi:10.14806/ej.17.1.200.

Mizuno, C. M., F. Rodriguez-Valera, and R. Ghai (2015), Genomes of planktonic *Acidimicrobiales*: Widening horizons for marine *Actinobacteria* by metagenomics, *MBio*, *6*(1), 1–11, doi:10.1128/mBio.02083-14.

Muyzer, G., E. C. De Waal, and A. G. Uitterlinden (1993), Profiling of complex microbial populations by denaturing gradient gel electrophoresis analysis of polymerase chain reaction-amplified genes coding for 16S rRNA, *Appl. Environ. Microbiol.*, *59*(3), 695–700.

Nicolsky, D. J., V. E. Romanovsky, N. N. Romanovskii, A. L. Kholodov, N. E. Shakhova, and I. P. Semiletov (2012), Modeling sub-sea permafrost in the East Siberian Arctic Shelf: The Laptev Sea region, *J. Geophys. Res.*, *117*, F03028, doi:10.1029/2012JF002358.

Nobu, M. K., et al. (2016), Phylogeny and physiology of candidate phylum "Atribacteria" (OP9/JS1) inferred from cultivation-independent genomics, *ISME J.*, *10*(2), 273–286, doi:10.1038/ismej.2015.97.

Normand, P., D. Daffonchio, and M. Gtari (2014), The family *Geodermatophilaceae*, in *The Prokaryotes*, pp. 361–379, Springer, Berlin, Germany.

Oren, A., and X.-W. Xu (2014), The family *Hyphomicrobiaceae*, in *The Prokaryotes*, pp. 247–281, Springer, Berlin, Germany.

Osterkamp, T. E. (2001), Sub-sea permafrost, in *Elements of Physical Oceanography: A Derivative of the Encyclopedia of Ocean Sciences*, vol. 2, edited by J. H. Steele, S. A. Thorpe, and K. K. Turekian, pp. 2902–2912, Academic Press, Cambridge, Mass.

Overduin, P. P., V. Rachold, and M. N. Grigoriev (2008), The state of subsea permafrost in the western Laptev nearshore zone, in *Proceedings of the Ninth International Conference on Permafrost*, pp. 1345–1350, Faribanks, Alaska.

Overduin, P. P., S. Liebner, C. Knoblauch, F. Günther, S. Wetterich, L. Schirrmeister, H. W. Hubberten, and M. N. Grigoriev (2015), Methane oxidation following submarine permafrost degradation: Measurements from a central Laptev Sea shelf borehole, *J. Geophys. Res. Biogeosci.*, *120*, 965–978, doi:10.1002/2014JG002862.

Overduin, P. P., S. Wetterich, F. Günther, M. N. Grigoriev, G. Grosse, L. Schirrmeister, H. W. Hubberten, and A. Makarov (2016), Coastal dynamics and submarine permafrost in shallow water of the central Laptev Sea, East Siberia, *Cryosphere*, *10*(4), 1449–1462, doi:10.5194/tc-10-1449-2016.

Parkes, R. J., H. Sass, B. A. Cragg, G. Webster, E. G. P. Roussel, and A. J. Weightman (2014), Studies on prokaryotic populations and processes in subseafloor sediments—an update, in *Microbial Life of the Deep Biosphere*, edited by J. Kallmeyer and D. Wagner, pp. 1–27, de Gruyter, Berlin, Germany.

Portnov, A., A. J. Smith, J. Mienert, G. Cherkashov, P. Rekant, P. Semenov, P. Serov, and B. Vanshtein (2013), Offshore permafrost decay and massive seabed methane escape in water depths >20 m at the South Kara Sea shelf, *Geophys. Res. Lett.*, *40*, 3962–3967, doi:10.1002/grl.50735.

Rachold, V., D. Y. Bolshiyanov, M. N. Grigoriev, H.-W. Hubberten, R. Junker, V. V. Kunitsky, F. Merker, P. Overduin, and W. Schneider (2007), Nearshore Arctic subsea permafrost in transition, *Eos Trans. AGU*, *88*(13), 149–150, doi:10.1029/2007EO130001.

Rietz, D. N., and R. J. Haynes (2003), Effects of irrigation-induced salinity and sodicity on soil microbial activity, *Soil Biol. Biochem.*, *35*(6), 845–854, doi:10.1016/S0038-0717(03)00125-1.

Rinke, C., et al. (2013), Insights into the phylogeny and coding potential of microbial dark matter, *Nature*, *499*(7459), 431–437, doi:10.1038/nature12352.

Rivkina, E. M., E. I. Friedmann, and C. P. Mckay (2000), Metabolic activity of permafrost bacteria below the freezing point, *Appl. Environ. Microbiol.*, *66*(8), 3230–3233, doi:10.1128/AEM.66.8.3230-3233.2000.Updated.
Romanovskii, N. N., and H.-W. Hubberten (2001), Results of permafrost modelling of the lowlands and shelf of the Laptev Sea Region, Russia, *Permafr. Periglac. Processes*, *12*(2), 191–202, doi:10.1002/ppp.387.
Romanovskii, N. N., H. W. Hubberten, A. V. Gavrilov, A. A. Eliseeva, and G. S. Tipenko (2005), Offshore permafrost and gas hydrate stability zone on the shelf of East Siberian Seas, *Geo-Mar. Lett.*, *25*(2–3), 167–182, doi:10.1007/s00367-004-0198-6.
Schirrmeister, L. (2007), Expeditions in Siberia in 2005, Russian-German Cooperation System LAPTEV SEA: The Expedition Coast I. The Expedition Lena 2005, in *Berichte zur Polar- und Meeresforschung = Reports on Polar and Marine Research*, 289 pp.
Schirrmeister, L., et al. (2008), Periglacial landscape evolution and environmental changes of Arctic lowland areas for the last 60000 years (western Laptev Sea coast, Cape Mamontov Klyk), *Polar Res.*, *27*(2), 249–272, doi:10.1111/j.1751-8369.2008.00067.x.
Schirrmeister, L., G. Schwamborn, P. P. Overduin, J. Strauss, M. C. Fuchs, M. Grigoriev, I. Yakshina, J. Rethemeyer, E. Dietze, and S. Wetterich (2016), Yedoma Ice Complex of the Buor Khaya Peninsula (southern Laptev Sea), *Biogeosci. Discuss.*, 1–36, doi:10.5194/bg-2016-283.
Schmidt, T. M. (1998), Multiplicity of ribosomal RNA operons in prokaryotic genomes, in *Bacterial Genomes*, pp. 221–229, Springer, Boston, Mass.
Schuur, E. A. G., A. D. McGuire, G. Grosse, J. W. Harden, D. J. Hayes, G. Hugelius, C. D. Koven, and P. Kuhry (2015), Climate change and the permafrost carbon feedback, *Nature*, *520*, 171–179, doi:10.1038/nature14338.
Schuur, E. A. G., J. G. Vogel, K. G. Crummer, H. Lee, J. O. Sickman, and T. E. Osterkamp (2009), The effect of permafrost thaw on old carbon release and net carbon exchange from tundra, *Nature*, *459*(7246), 556–559, doi:10.1038/Nature08031.
Shakhova, N., I. Semiletov, A. Salyuk, V. Yusupov, D. Kosmach, and Ö. Gustafsson (2010), Extensive methane venting to the atmosphere from sediments of the East Siberian Arctic Shelf, *Science*, *327*, 1246–1250, doi:10.1126/science.1229223.
Shakhova, N., et al. (2014), Ebullition and storm-induced methane release from the East Siberian Arctic Shelf, *Nat. Geosci.*, *7*, 64–70, doi:10.1038/ngeo2007.
Steven, B., G. Briggs, C. P. McKay, W. H. Pollard, C. W. Greer, and L. G. Whyte (2007), Characterization of the microbial diversity in a permafrost sample from the Canadian high Arctic using culture-dependent and culture-independent methods, *FEMS Microbiol. Ecol.*, *59*(2), 513–523, doi:10.1111/j.1574-6941.2006.00247.x.
Stokstad, E. (2003), Ancient DNA pulled from soil, *Science*, *300*(5618), 407a, doi:10.1126/science.300.5618.407a.
Svendsen, J. I., et al. (2004), Late Quaternary ice sheet history of northern Eurasia, *Quat. Sci. Rev.*, *23*(11–13), 1229–1271, doi:10.1016/j.quascirev.2003.12.008.
Thornton, B. F., M. C. Geibel, P. M. Crill, C. Humborg, and C. M. Mörth (2016), Methane fluxes from the sea to the atmosphere across the Siberian shelf seas, *Geophys. Res. Lett.*, *43*, 5869–5877, doi:10.1002/2016GL068977.
Ulyantsev, A. S., N. V. Polyakova, E. A. Romankevich, I. P. Semiletov, and V. I. Sergienko (2016), Ionic composition of pore water in shallow shelf deposits of the Laptev Sea, *Dokl. Earth Sci.*, *467*(1), 308–313, doi:10.1134/S1028334X16030211.
Wagner, D., A. Gattinger, A. Embacher, E.-M. Pfeiffer, M. Schloter, and A. Lipski (2007), Methanogenic activity and biomass in Holocene permafrost deposits of the Lena Delta, Siberian Arctic and its implication for the global methane budget, *Global Change Biol.*, *13*(5), 1089–1099, doi:10.1111/j.1365-2486.2007.01331.x.
Waldrop, M. P., K. P. Wickland, R. White, A. A. Berhe, J. W. Harden, and V. E. Romanovsky (2010), Molecular investigations into a globally important carbon pool: Permafrost-protected carbon in Alaskan soils, *Global Change Biol.*, *16*(9), 2543–2554, doi:10.1111/j.1365-2486.2009.02141.x.
Wang, Y., H. F. Sheng, Y. He, J. Y. Wu, Y. X. Jiang, N. F. Y. Tam, and H. W. Zhou (2012), Comparison of the levels of bacterial diversity in freshwater, intertidal wetland, and marine sediments by using millions of Illumina tags, *Appl. Environ. Microbiol.*, *78*(23), 8264–8271, doi:10.1128/AEM.01821-12.
Wegner, C., J. A. Hölemann, I. Dmitrenko, S. Kirillov, and H. Kassens (2005), Seasonal variations in Arctic sediment dynamics—Evidence from 1-year records in the Laptev Sea (Siberian Arctic), *Global Planet. Change*, *48*(1–3), 126–140, doi:10.1016/j.gloplacha.2004.12.009.
Willerslev, E., A. J. Hansen, R. Rønn, T. B. Brand, I. Barnes, C. Wiuf, D. Gilichinsky, D. Mitchell, and A. Cooper (2004), Long-term persistence of bacterial DNA, *Curr. Biol.*, *14*(1), 13–14, doi:10.1016/j.cub.2003.12.012.
Winterfeld, M., L. Schirrmeister, M. N. Grigoriev, V. V. Kunitsky, A. Andreev, A. Murray, and P. P. Overduin (2011), Coastal permafrost landscape development since the Late Pleistocene in the western Laptev Sea, Siberia, *Boreas*, *40*(4), 697–713, doi:10.1111/j.1502-3885.2011.00203.x.
Yi, H., and J. Chun (2004), *Nocardioides aestuarii* sp. nov., isolated from tidal flat sediment, *Int. J. Syst. Evol. Microbiol.*, *54*(6), 2151–2154, doi:10.1099/ijs.0.63192-0.
Zhang, D. F., J. M. Zhong, X. M. Zhang, Z. Jiang, E. M. Zhou, X. P. Tian, S. Zhang, and W. J. Li (2014), *Nocardioides nanhaiensis* sp. nov., an actinobacterium isolated from a marine sediment sample, *Int. J. Syst. Evol. Microbiol.*, *64*(8), 2718–2722, doi:10.1099/ijs.0.062851-0.
Zhang, J., K. Kobert, T. Flouri, and A. Stamatakis (2014), PEAR: A fast and accurate Illumina paired-end reAd mergeR, *Bioinformatics*, *30*(5), 614–620, doi:10.1093/bioinformatics/btt593.
Zhang, T., R. G. Barry, K. Knowles, J. A. Heginbottom, and J. Brown (1999), Statistics and characteristics of permafrost and ground-ice distribution in the Northern Hemisphere, *Polar Geogr.*, *23*(2), 132–154, doi:10.1080/10889379909377670.
Zhou, J., M. A. Bruns, and J. M. Tiedje (1996), DNA recovery from soils of diverse composition, *Appl. Environ. Microbiol.*, *62*(2), 316–322.